Journal of Renewable and Sustainable Energy

Hydrokinetic energy conversion: A global riverine perspective

Cite as: J. Renewable Sustainable Energy **14**, 044501 (2022); https://doi.org/10.1063/5.0092215
Submitted: 22 March 2022 • Accepted: 28 June 2022 • Accepted Manuscript Online: 29 June 2022 • Published Online: 22 July 2022

Published open access through an agreement with JISC Collections

Michael Ridgill, Matt J. Lewis, Peter E. Robins, et al.

Journal of Renewable and Sustainable Energy ARTICLE scitation.org/journal/rse

Hydrokinetic energy conversion: A global riverine perspective

Cite as: J. Renewable Sustainable Energy **14**, 044501 (2022); doi: 10.1063/5.0092215
Submitted: 22 March 2022 · Accepted: 28 June 2022 ·
Published Online: 22 July 2022

View Online Export Citation CrossMark

Michael Ridgill,[1,a)] Matt J. Lewis,[1] Peter E. Robins,[1] Sopan D. Patil,[2] and Simon P. Neill[1]

AFFILIATIONS

[1]School of Ocean Sciences, Bangor University, Menai Bridge LL59 5AB, United Kingdom
[2]School of Natural Sciences, Bangor University, Bangor LL57 2UW, United Kingdom

[a)]Author to whom correspondence should be addressed: m.a.ridgill@bangor.ac.uk

ABSTRACT

Free-flowing rivers have been impacted by anthropogenic activity and extensive hydropower development. Despite this, many opportunities exist for context-specific energy extraction, at locations deemed undesirable for conventional hydropower plants, in ways that reduce the scale of operation and impact. Hydrokinetic energy conversion is a renewable energy technology that requires accurate resource assessment to support deployment in rivers. We use global-scale modeled river discharge data, combined with a high-resolution vectorized representation of river networks, to estimate channel form, flow velocities, and, hence, global hydrokinetic potential. Our approach is based directly on the transfer of kinetic energy through the river network, rather than conventional, yet less realistic, assessments that are based on conversion from gravitational potential energy. We show that this new approach provides a more accurate global distribution of the hydrokinetic resource, highlighting the importance of the lower-courses of major rivers. The resource is shown to have great potential on the continents of South America, Asia, and Africa. We calculate that the mean hydrokinetic energy of global rivers (excluding Greenland and Antarctica) is 5.911 ± 0.009 PJ (1.642 ± 0.003 TWh).

I. INTRODUCTION

The energy within water is apparent in the propagation of gravity waves, density gradients, the gravitational potential energy attained through elevation change, or as kinetic energy due to its movement. The latter two examples are of most relevance to rivers, where the conversion of gravitational potential energy can be described as hydrostatic and kinetic energy conversion as hydrokinetic.[1] The hydrostatic approach is commonly exploited by impounding a reservoir of gravitational potential energy, as a hydraulic head behind a dam, as in conventional hydropower plants. The hydrokinetic approach involves directly converting the "free stream" kinetic energy of flowing water. Hydrokinetic energy conversion (HEC) specifically refers to the conversion of the kinetic energy contained in river streams, tidal currents, or artificial waterways, for the generation of electricity through the installation of in-stream turbines.[2]

With a global installed capacity estimated to be 1.3 TW, conventional hydropower accounts for ∼16% of global electricity production, generating more electricity than any other renewable energy technology.[3,4] Despite providing large amounts of electricity, the development of hydropower has raised serious social, environmental, and economic concerns,[5–9] with some questioning the justification for continued development.[6,8,9] Furthermore, from a political, practical, and economic perspective, future hydropower plant constructions may be either technically, or economically, infeasible.[5,10] Perhaps indicative of a change in sentiment more widely, Punys *et al.*[1] have described the limitations put on further development of hydropower, in Lithuania, and administrative preference moving more in the direction of less impactful renewable energy technologies, including HEC. Resource assessment in support of these technologies, therefore, becomes more necessary. Also, given the current importance of hydropower, increased extraction of hydrokinetic energy will necessitate consideration of the impact upon existing hydropower installation in which this resource assessment can support.

HEC is relatively immature, especially when compared with other renewable energy technologies such as hydropower, wind, and solar, with resource assessment identified as one of the main challenges hindering its commercial rollout.[2,11] Few regional- to large-scale resource assessments exist for HEC in rivers.[12–16] Such assessments are challenging, due to the dominant influence of flow velocity for this technology. Given its dependence upon the complicated

interaction of many other factors, flow velocity is highly sensitive and variable.[17] It is, therefore, difficult to estimate the HEC resource without direct measurement over extended time periods. Improved knowledge of the hydrokinetic resource within rivers provides a more complete assessment of the global potential for HEC and addresses the need for large-scale hydrokinetic resource assessment.

A theoretical resource assessment, in contrast to technical or practical resource assessments, quantifies the total energy that is hypothetically available for conversion, without consideration of feedbacks between extraction and the resource.[18] Previous theoretical resource assessments of HEC have adopted an approach that considers power as the rate of energy conversion from gravitational potential energy to kinetic energy.[15,16] This is more appropriate from a hydrostatic perspective and implies unrealistically high flow speeds that would not naturally occur in river channels. In this paper, we have derived a novel methodology that instead considers power as the direct rate of transfer of kinetic energy through river reaches. Estimation of channel form and flow velocity is achieved using established power law relationships,[19] with numerical constants that are considered to be globally applicable.[20] Uncertainties associated with these numerical constants, which are asymmetrical and would lead to an underestimation bias, are addressed using a Monte Carlo method. Thus, in support of the development of HEC, we offer a theoretical resource assessment that benefits from a perspective that is hydrokinetic rather than hydrostatic.

A. The conventional approach to hydrokinetic resource assessment

In previous hydrokinetic resource assessments,[15,16] theoretical hydraulic power P has been calculated using

$$P = \gamma Q H, \tag{1}$$

where γ is the specific weight of water (9800 N m^{-3}), Q is the discharge (volumetric flow rate), and H is the change in elevation of a given river section. This equation can be derived from a consideration of gravitational potential energy E_p, using the classical equation:

$$E_p = MgH, \tag{2}$$

where M is the mass of water and g is the acceleration due to gravity. Since M is the product of density ρ and volume V,

$$E_p = \rho V g H, \tag{3}$$

where P is the rate of energy conversion and $Q = V/t$ is the volumetric flow rate. Therefore, dividing by time t gives

$$P = \rho Q g H. \tag{4}$$

Given that $\gamma = \rho g$, this demonstrates the derivation of Eq. (1). Considering this derivation, Eq. (1) is relevant from a hydrostatic, rather than a hydrokinetic, perspective. A methodology that focuses on flow velocity—to reflect a technology (hydrokinetic energy conversion) that uses the energy of free-flowing water directly, rather than a technology (conventional hydropower) that uses the impoundment of a hydraulic head—may be more appropriate. To support this argument, consider the quantification of power output by conventional hydropower, derived from a consideration of kinetic energy E_k, as defined by the classical equation:

$$E_k = \frac{1}{2} M v^2, \tag{5}$$

where v is the velocity. Power is the rate of energy transfer

$$P = \frac{dE_k}{dt}. \tag{6}$$

Using the product rule for derivatives gives

$$P = \frac{1}{2}\left(v^2 \frac{dM}{dt} + M \frac{dv^2}{dt}\right). \tag{7}$$

When considering a flowing fluid, Bernoulli's equation[21] states that

$$E_p + E_k + U = \text{constant}, \tag{8}$$

where U is the internal energy. If considered per unit volume, this can be expressed as

$$\frac{1}{2}\rho v^2 + \rho g z + p = \text{constant}, \tag{9}$$

where z is the elevation of the point above a reference plane and p is the pressure.

The conservation of energy means that there can be no loss of energy as the fluid flows between two points. Therefore, if considering fluid at the surface of a body of water constrained behind a dam and fluid flowing through a penstock at the base of the dam (Fig. 1), this can be described with

$$\frac{1}{2}\rho v_1^2 + \rho g z_1 + p_1 = \frac{1}{2}\rho v_2^2 + \rho g z_2 + p_2. \tag{10}$$

A fluid flowing through the penstock located at a height defined as $z_2 = 0$ will have a velocity v_2. The surface is elevated above this at z_1, where the velocity of the fluid is $v_1 = 0$. Due to the surface and the outlet of the penstock being acted upon by atmospheric pressure, $p_1 = p_2$. Now,

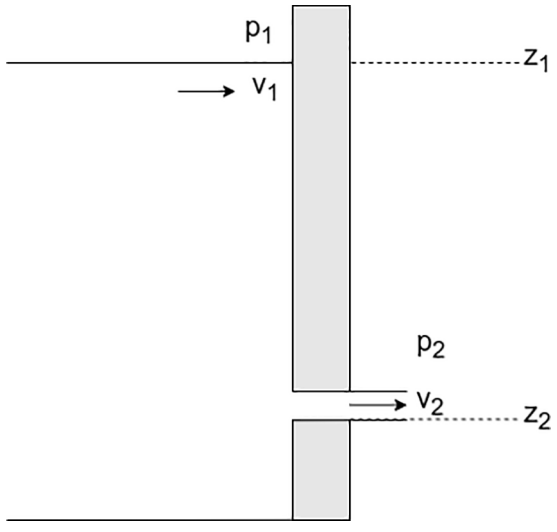

FIG. 1. The pressure p, elevation z, and flow velocity v of a fluid at the surface behind a dam and flowing through a penstock at the base of the dam.

$$\frac{1}{2}\rho v_2^2 = \rho g z_1, \tag{11}$$

which rearranges to give

$$v_2 = \sqrt{2gz_1}. \tag{12}$$

More generally, the velocity of a fluid leaving a container, or a dam, is given by

$$v = \sqrt{2gH}, \tag{13}$$

where, in this case, $H = z_1 - z_2$ represents the change in elevation from the penstock to the surface of the water impounded behind the dam but is equivalent to the earlier definition of H. Since g and H remain constant, so does v, meaning

$$\frac{dv^2}{dt} = 0. \tag{14}$$

The rate of change of mass is

$$\frac{dM}{dt} = Q\rho. \tag{15}$$

Substituting for Eqs. (14) and (15) into Eq. (7) gives

$$P = \frac{1}{2} \cdot 2gH \cdot Q\rho. \tag{16}$$

Since $\gamma = \rho g$, this derivation from a consideration of kinetic energy agrees with the derivation of the equation for calculating power from a consideration of gravitational potential energy [Eq. (1)].

Implicit in Bernoulli's principle is the idea that energy is conserved throughout a body of water. This means that the energy that a particle of water at the bottom of a column of water is equal to the energy at the top of the water column. This is analogous to the conservation of energy that is exhibited by a body in free fall, as gravitational potential energy is converted into kinetic energy. Therefore, if ignoring all forms of friction, the velocity of the water released from below the surface of a body of water (Fig. 1) can be determined by consideration of the equation of motion, from classical physics,

$$v_f^2 = v_0^2 + 2a(r - r_0), \tag{17}$$

where v_f is a particle's final velocity, v_0 is the initial velocity, a is the acceleration, r is the final position, and r_0 is the initial position. (This is also commonly stated as $v^2 = u^2 + 2as$.) With reference to Fig. 1, $v_f = v_2$, $v_0 = v_1 = 0$, $a = -g$, and $r - r_0 = z_2 - z_1$. Therefore, this becomes

$$v_2^2 = v_1^2 - 2g(z_2 - z_1). \tag{18}$$

If we assign a value for the height of water above the point of exit, such that $H = z_1 - z_2$, this gives

$$v^2 = 2gH, \tag{19}$$

which can be rearranged to give Eq. (13). To illustrate what this means, an object released outside of the body of water and from the top of the container (at height z_1) will reach the same velocity in free fall (if excluding air resistance), when arriving at the bottom of the container, as the water released at the bottom of the container.

The power available from HEC is modest compared to that from conventional hydropower. To illustrate this, Eq. (13) can be used to show that a flow speed of 1 ms^{-1} would correspond to a static head height of only 50 mm. Therefore, even a modestly sized conventional impoundment hydropower plant can theoretically result in a considerable flow speed (Fig. 2).

The dataset used in this study includes river reaches with a median (mean) length of 6.8 km (9.2 km) but ranges between 0.01–424.67 km. The maximum change in elevation for a reach within this dataset is $H = 3734$ m. This corresponds to a flow velocity of $v = 271$ ms^{-1}, after applying Eq. (13). This is clearly unreasonably high, given that such a flow velocity is unrealistic.

Power is a measure of the rate of energy conversion, or the rate of energy transfer. Using the conventional equation [Eq. (1)] to calculate the theoretical hydrokinetic resource within a given reach, means considering the conversion from gravitational potential energy to kinetic energy that theoretically occurs within a reach. Of course, energy will be dissipated by friction against the bed and banks of this reach, in practice, but using this method of theoretical resource assessment means any friction is discounted. This point is confirmed by remembering the means of derivation of Eq. (1) and how Q is essentially a measure of the quantity of water, rather than a measure of volumetric flow rate, in this context. This method does not acknowledge a movement of water at all, in fact, only the change in energy that occurs, in a given mass of water, due to a change in elevation. Still, in practical terms, using the conventional equation implies unrealistic values for v as calculated by Eq. (13) and illustrated in Fig. 2. As will be discussed below, the dissipation of energy by friction is not equal throughout a river, from the upper- to the lower-courses. Therefore, the use of the conventional equation, even if accounting for the fact that friction is omitted, may still be biased according to the position in a river network considered and provide an unrealistic perspective on the global distribution of HEC potential.

Furthermore, this approach implies that as the slope reduces, v will decrease. This is a common misconception and the opposite of what actually occurs. As we shall explain further below, Leopold and Maddock[19] predict an increase in v with an increase in Q [Eq. (25)]. As you proceed downstream, Q will tend to increase because the drainage area progressively increases. Only in exceptional cases, particularly in arid areas, will rivers have Q decrease in a downstream direction.

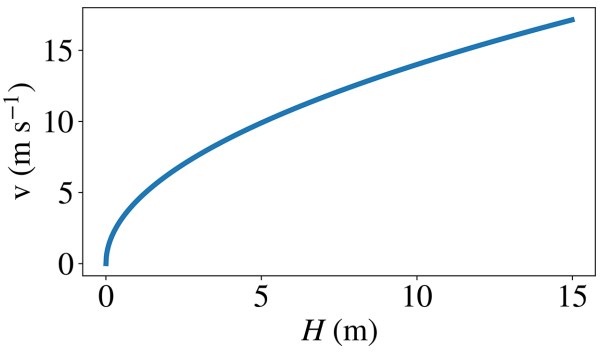

FIG. 2. The conversion of gravitational potential energy to kinetic energy implies that flow velocity $v = \sqrt{2gH}$, when considered using Bernoulli's principle.

The upper-courses of a river flow down from high hills and mountains. They are often narrow, steep, and marked by sharp valleys and abrupt changes of direction. The steepness means that there is much gravitational potential energy, often resulting in high turbulence, waterfalls, and high levels of erosion. Upland streams can appear to have very fast flows; however, this is usually very turbulent, and in fact, much of the water in the upper-course is almost stationary, particularly close to the bed and banks where friction is highest. The transition from upper- to middle-courses is marked by a widening of channels and reduced steepness. The lower-courses can be similar to the middle-courses but generally wider and less steep.

The Manning formula gives another means for determining v, using

$$v = \frac{R^{\frac{2}{3}} s^{\frac{1}{2}}}{n}, \tag{20}$$

where R is the hydraulic radius, s is the slope, and n is the Manning roughness coefficient. The hydraulic radius is given by

$$R = \frac{A}{W}, \tag{21}$$

where A is the cross-sectional area and W is the wetted perimeter. Both will increase in a downstream direction, but the rate of increase in A is greater than W, causing R to increase downstream. Though the relative change in magnitude of s and R cannot be quantified in general terms, apart from the likelihood that s will decrease and R will increase, it is important to notice that in Eq. (20), the exponent for R is greater than that for s. Therefore, moving downstream, the increase in R will have more affect than the decrease in s. This may be interpreted as meaning that the decrease in boundary-induced friction overcompensates for the decrease in slope. An increase in v in a downstream direction is also confirmed by the Bradshaw model.[22,23]

A method of hydrokinetic resource assessment that focuses directly on the transfer of kinetic energy, rather than the conversion of gravitational potential energy to kinetic energy, potentially offers a more realistic and pragmatically useful approach. We look to identify if this provides a meaningfully different, relevant, and useful perspective, with sufficient evidence to support this being more accurate and representative of the riverine hydrokinetic resource.

II. METHODS

A. Data

Global Reach-level A *priori* Discharge Estimates (GRADES) is a 35 year (1979–2013) reconstructed record of daily values for river discharge Q, with rivers split up into ∼3 million individual reaches of mean (median) length of 9.2 km (6.8 km).[24] Use of the Variable Infiltration Capacity (VIC) macroscale hydrologic model[25,26] and the Routing Application for Parallel computatIon of Discharge (RAPID) river routing model,[27] in the construction of GRADES, permits representation of ungaged rivers in this model. Machine learning algorithms and empirical data, from over 14 000 gauges and a number of globally distributed organizations, were used to calibrate this method, and when evaluated against this gauged data, Lin *et al.*[24] report that 35% (64%) have a percentage bias within ±20% (±50%). These error measurements, therefore, impact upon any results that our methodology produces. Multi-Error-Removed-Improved-Terrain (MERIT) Hydro is a hydrography map that provides a framework within which GRADES has been constructed, providing high-resolution, vectorized, global flow direction maps at 3-arc sec resolution (∼90 m at the equator).[28] MERIT Hydro was derived from elevation data, provided by Multi-Error-Removed-Improved-Terrain Digital Elevation Model (MERIT DEM),[29] combined with water body datasets, including G1WBM,[30] Global Surface Water Occurrence,[31] and OpenStreetMap. The use of water layer datasets enables an improvement of the elevation measurements of MERIT DEM because pixels with higher estimated probability of water occurrence will be expected to have a lower elevation than adjacent pixels with lower estimated probability. OpenStreetMap helps to represent small streams not visible at low resolution.

Compared against existing products,[32,33] this global hydrography dataset provides a more realistic depiction of river flowlines than has ever been achieved, a better representation of small streams, not visible in 1-arc sec (∼30 m at the equator) resolution Landsat data, and coverage above 60°N. Previous hydrography maps have used high-resolution raster grids, with pixels to represent flow accumulation. Small streams have, therefore, not been resolved if their width is smaller than the pixel size. Supplementary material can be used to improve a hydrography map at the regional-scale[34] but this is not practical at the continental- or global-scale. Prior to MERIT Hydro, HydroSHEDS was the only global-scale high-resolution hydrography map available, and it required a great deal of manual editing.[32] Locations of small rivers in HydroSHEDS were not well represented. This is especially true in forested areas, due to elevation errors caused by tree canopies.

GRADES is divided up into 9 Level 1 continental-level divisions, according to the Pfafstetter system,[35] representing the global river network (Fig. 3). GRADES does not include discharge data for the Greenland continental-level division, at this time, due to a lack of sufficient training and validation data (Pan, co-author of Lin *et al.*[24] Pers. Comm.). Greenland accounts for 42 246 of the total 2 940 747 reaches, or 1.4%. When the length of all reaches is summed, Greenland accounts for 2.5%. Antarctica is not considered in this dataset. The Antarctic hydrological system consists of superglacial lakes, subsurface lakes, surface streams, and rivers that function quite differently to the terrestrial hydrological systems that makeup the vast majority of the global network of rivers.[36]

B. Hydrokinetic power as the rate of energy transfer

Theoretical power can be considered flowing through a river cross section, using

$$P = \frac{1}{2}\rho A v^3. \tag{22}$$

This equation is derived from kinetic energy, which will be demonstrated below. It is also applicable to determine the power of water passing a turbine. In this context, A refers to the cross-sectional area of the sweep of the turbine. Applying Eq. (22) to rivers requires knowledge of width w, depth d, and the cross-sectional profile (to calculate A), in addition to knowing v. Large-scale resource assessments face the challenge of obtaining suitable data, with appropriate coverage and spatiotemporal resolution. Relatively limited empirical information on river channel form is available at a continental-scale,[37] and v is highly variable in time and space.[38] With modeled data for reconstructed daily values of Q, GRADES provides near-global coverage and may be

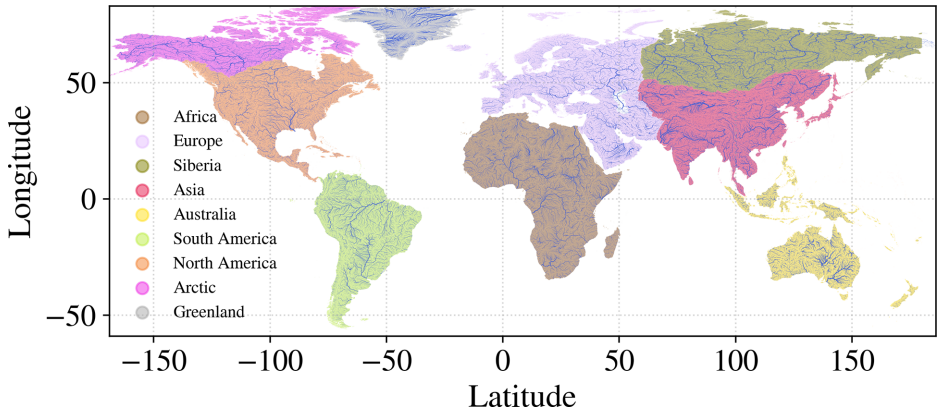

FIG. 3. Level 1 continental-level divisions as defined by the Pfafstetter coding system.

applicable in estimating appropriate values to determine river channel form and v.

Assuming that Q is the dominant independent variable, Leopold and Maddock[19] proposed that the hydraulic geometry of a fluvial channel can be described, using power law relationships, as functions of Q,

$$w = aQ^b, \tag{23}$$

$$d = cQ^f, \tag{24}$$

$$v = kQ^m, \tag{25}$$

where the parameters a, b, c, f, k, and m are empirically determined numerical constants that vary with location, climate, and discharge conditions. The equations for describing hydraulic geometry can be applied at-a-station, or downstream, providing two approaches for empirically determining these parameters. Confusingly, Leopold and Maddock[19] used the same variables and naming conventions to describe at-a-station hydraulic geometry (AHG) and downstream hydraulic geometry (DHG). The AHG approach requires repeated field-measurements at a single cross section. The DHG approach requires repeated field-measurements at a fixed frequency of discharge between cross sections, either downstream or on other rivers. These relationships for estimating w, d, and v provide the possibility to derive an alternative methodology for hydrokinetic resource assessment.

Power is the rate of energy transfer

$$P = \frac{E_k}{t} = \frac{\frac{1}{2}Mv^2}{t}. \tag{26}$$

The dimensions of a river reach can be approximately described as a rectangular shaped channel, which serves our purposes for now, using hydraulic geometry parameters w, d, and the length of the reach L (Fig. 4). The power of the water moving in this reach can be expressed in terms of these dimensions. Since M is the product of ρ and volume $V = wdL$, in relation to the water in a reach, this gives

$$M = \rho wdL. \tag{27}$$

Substituting for M in Eq. (26) gives

$$P = \frac{\frac{1}{2}\rho wdLv^2}{t}. \tag{28}$$

Since

$$v = \frac{L}{t}, \tag{29}$$

this simplifies to

$$P = \frac{1}{2}\rho wdv^3. \tag{30}$$

Since $A = wd$, this confirms the derivation of Eq. (22). Substituting for w, d, and v using Eqs. (23)–(25) gives

$$P = \frac{1}{2}\rho \cdot aQ^b \cdot cQ^f \cdot (kQ^m)^3. \tag{31}$$

Discharge is defined as the volume of water that passes through a cross section. Therefore,

$$Q = wdv = aQ^b \cdot cQ^f \cdot kQ^m = ackQ^{b+f+m}. \tag{32}$$

This demonstrates that

$$ack = 1 \tag{33}$$

and

$$b + f + m = 1, \tag{34}$$

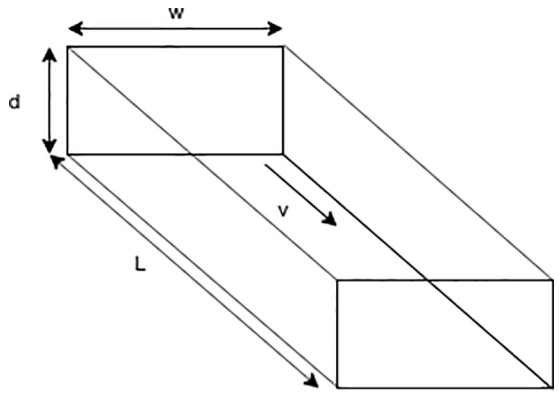

FIG. 4. Approximate description of a river section of length L, using the hydraulic geometry parameters of width w, depth d, and flow velocity v.

which means power can be expressed as

$$P = \frac{1}{2}\rho k^2 Q^{(2m+1)}. \quad (35)$$

Threshold theory developed from a determination that the stability of irrigation canals, constructed with erodible materials, is optimum with cross sections that cause material to be at the threshold of motion.[39] This was shown to apply to natural rivers as well.[40] With particles on the verge of movement at bankfull discharge, a resolution of the associated forces yields a cross section that is roughly parabolic in shape.[41] The cross-sectional form of natural channels is irregular, but a parabolic shape is used here to generalize on a global-scale. The area of a parabolic cross section is given by

$$A = \frac{2}{3}wd. \quad (36)$$

Applying this to Eq. (35) and remembering that this was arrived at through a derivation that originally included w and d [Eq. (30)], we get an equation for determining the power of water flowing through a parabolic channel cross section

$$P = \frac{1}{3}\rho k^2 Q^{(2m+1)}. \quad (37)$$

We consider this equation an alternative to the conventionally used equation [Eq. (1)] for determining theoretical hydraulic power and potentially more suitable for a hydrokinetic application. This can be modified to measure the energy E that flows through a river reach by multiplying through by t. With reference to Eq. (29), this gives

$$E = \frac{1}{3}\rho LkQ^{(m+1)}. \quad (38)$$

C. Globally applicable power law parameters

Moody and Troutman[20] used regression analysis upon a number of studies of rivers to determine values for the power law parameters in Eqs. (23) and (24). This analysis enabled the proposal of globally applicable formulas for the estimation of w and d, using

$$w = 7.2Q^{0.50\pm0.02} \quad (2.6 - 20.2), \quad (39)$$

$$d = 0.27Q^{0.30\pm0.01} \quad (0.12 - 0.63), \quad (40)$$

with the numbers in parentheses corresponding to the 95% confidence interval for the coefficients. The regression standard error of estimate for Eqs. (39) and (40) is 0.22 and 0.18, respectively. These authors state that the estimate of the coefficients and exponents would probably change little with more data because the number of data pairs is 226 and includes measurements for some of the largest rivers in the world and many of the smallest. As shown, the coefficients tend to vary more than the exponents, reflecting the multivariate character of the channel form control. Though these relationships and parameters have been assumed globally applicable by other studies,[24,37,42–45] they are not strictly traditional hydraulic geometry relationships and do not adhere to either the AHG or DHG definitions. Moody and Troutman[20] justified their approach and argued that the range and quantity of data they used minimized the variability of the results.

Knowledge of a, b, c, and f allows the determination of k and m, using Eqs. (33) and (34). In this way, a globally applicable formula for v can be derived

$$v = 0.5Q^{0.20\pm0.03} \quad (0.1 - 3.2). \quad (41)$$

It should be noted that v is one of the most sensitive and variable properties of open-channel flow, due to its dependence upon so many other factors. It varies in four dimensions: with time, with distance from the bed, across stream, and downstream. In addition to the variations due to changes in Q, smaller timescale variations also occur because of the inherent variability caused by turbulence. Friction from the bed and banks may result in large velocity gradients. These provisos are clearly stated in offering these globally applicable values for the parameters $m = 0.5$ (with a 95% confidence interval 0.1 to 3.2) and $k = 0.20 \pm 0.03$. A value of $m = 0.1$ has been proposed as appropriate previously.[46]

Figure 5 shows estimates of theoretical power as a function of Q using globally applicable power law parameters and assuming a rectangular cross-sectional profile. This illustrates that using Eq. (35) gives the same result as using Eq. (22), but with a reduced range of uncertainty. In the former case, only the parameters k and m are required. In the latter case, power law equations are used to estimate w, d, and v. Therefore, the parameters a, b, c, f, k, and m are needed.

In regard to their use of Eq. (39), Allen and Pavelsky[37] point out that this relationship was developed using measurements largely collected at gauging stations. Stream gauges are typically located at stable, single-channel sites, often near bridges or other fixed structures. This could lead to bias that is unrepresentative of global values for w. Since multichannel rivers tend to be wider and because their widths are more sensitive to variations in Q than single-channel rivers,[47] average river widths away from gauging stations may be underestimated. This opinion is reiterated elsewhere.[48,49]

Frasson *et al.*[50] compared modeled annual flow, simulated by the water balance model WBMsed,[51] with measurements of w obtained from remote sensing. They demonstrated that the power law relationship between w and Q, applied using the parameters proposed by Moody and Troutman[20] for a and b [Eq. (39)], showed close agreement with these measurements. They report that their observed disagreement at the lower end may be due to the increased uncertainty in the estimation of smaller river widths. A width of ∼50 m approaches

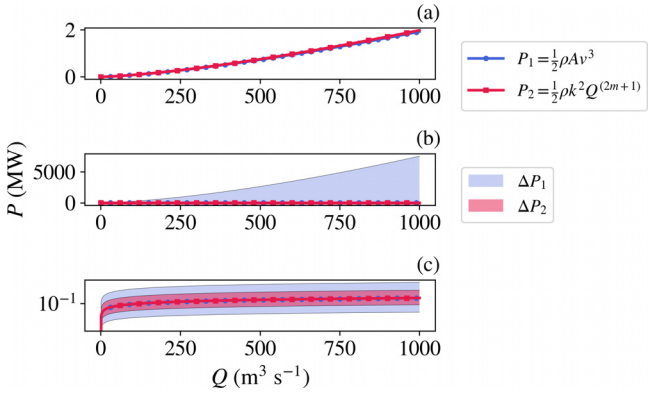

FIG. 5. In (a), the calculation of power is seen to be the same if using power law relationships that are functions of Q to estimate w, d, and v, to calculate $P_1 = \frac{1}{2}\rho A v^3$ (where $A = wd$), and the derived equation $P_2 = \frac{1}{2}\rho k^2 Q^{2m+1}$. The range of uncertainty ΔP_1 is seen to be greater than that for ΔP_2. Shown with (b) a linear scale and (c) a logarithmic scale on the y axis.

the 30 m resolution of the Landsat images used in the extraction of the river widths and may cause an overestimation.[37]

As shown in Fig. 5, the 95% confidence interval for the coefficients expressed in Eqs. (39)–(41) causes an asymmetrical uncertainty in estimates of power using Eqs. (22), (35), and (37), when applying power law parameters that we are treating globally applicable, for the purpose of estimating hydraulic geometry parameters. Given the uncertainties associated with these parameters, their statistical distribution within the rivers of the world can be assumed (Fig. 6).

Though it may be reasonable to use the mean values for these globally applicable power law parameters in estimating P for an individual reach, when considered collectively, the asymmetrical statistical distribution would lead to an underestimate of the collective power of a number of reaches, as is illustrated by Fig. 5.

D. Monte Carlo approach

The concept of repeated random sampling underlies the broad class of computational algorithms known as Monte Carlo methods. Though stochastic in nature, such methods can be used to solve problems that might be deterministic in principle. We use repeated ($n = 1000$), random application of power law parameters to each river reach, such that the collective statistical distribution for each run aligns with that implied by their reported uncertainties (Fig. 6). The mean of these repeated runs permits an estimate of the global theoretical riverine hydrokinetic resource, which reduces the effects of the asymmetric uncertainties and arguably results in a more accurate representation. The accuracy of the Monte Carlo method is proportional to $\sqrt{n}$, meaning that computation cost quadruples when accuracy is doubled.[52] In most cases, $n \geq 100$ is considered "best practice."[53]

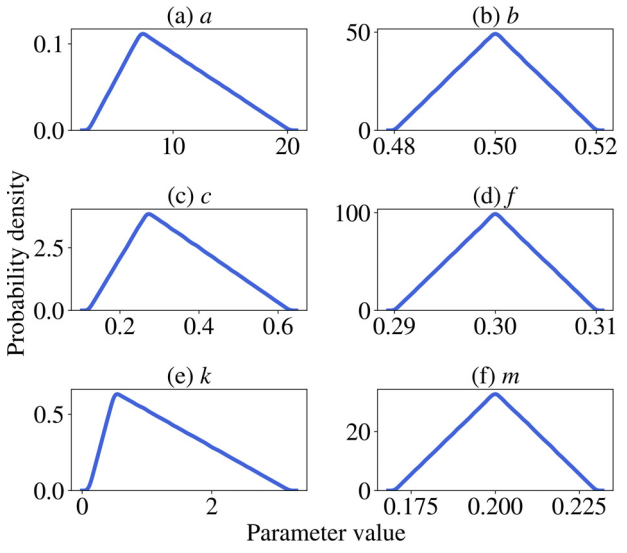

FIG. 6. Here, we illustrate the statistical distribution of the power law parameters, according to the reported and derived uncertainty. Leopold and Maddock[19] proposed power law relationships to estimate hydraulic geometry parameters, and Moody and Troutman[20] determined globally applicable coefficients and exponents for these power laws for width w [(a) and (b)] and depth d [(c) and (d)], including the associated uncertainty. Hydraulic geometry continuity has been used to derive power law parameters and uncertainty for flow velocity v [(e) and (f)].

Convergence tests provide a means to determine if the number of runs were sufficient and to quantify the reliability, or "stability," of a result. Here, $n = 1000$, and a measurement of the root mean square-error after each run is found to converge to almost zero (Fig. 7). In this case, over the 35 year record ($p = 12\,784$ days), a running mean vector $\vec{E}_{\mathrm{MC}}$ (Eq. (45)) gathered from a growing matrix of increasing numbers of completed runs $\mathbf{E}_{\mathrm{MC}} \in \mathbb{R}^{p \times n}$ for $n = 1, 2, 3, \ldots, 1000$ is calculated after each run and compared with the eventual mean vector for $n = 1000$. This is achieved by running the Monte Carlo method twice.

The equation derived to estimate the power within a given river reach [Eq. (37)] can be modified to measure the energy E that flows through a river reach by multiplying through by time [Eq. (38)]. This can be applied to all reaches simultaneously, meaning that we discretize each reach, such that they can be considered individually and summed to quantify the energy in all reaches collectively. All water within the global network of rivers can be thought of as flowing through one of these reaches and only one, when considered as a whole. The sum of these individual reaches is, therefore, the total energy of all reaches.

We can produce a vector $\vec{E}_{\mathrm{MP}}$, representing the daily total energy of all $q = 2\,898\,501$ river reaches, where mean power law parameters are applied for all reaches of length L. This is given by

$$\vec{E}_{\mathrm{MP},y} = \sum_{x=1}^{q} \frac{1}{3} \rho L_x k Q_{xy}^{(m+1)} \quad \text{where } \vec{E}_{\mathrm{MP}} \in \mathbb{R}^p. \tag{42}$$

Here, the mean globally applicable power law parameters are $k = 0.5$ and $m = 0.20$. The value $\bar{E}_{\mathrm{MP}}$ represents the mean energy of all river reaches over the time period, given by

$$\bar{E}_{\mathrm{MP}} = \frac{1}{p} \sum_{y=1}^{p} \sum_{x=1}^{q} \frac{1}{3} \rho L_x k Q_{xy}^{(m+1)} \quad \text{where } \bar{E}_{\mathrm{MP}} \in \mathbb{R}. \tag{43}$$

A vector $\vec{E}_{\mathrm{MC}}$ representing daily total energy of all reaches can be produced using random power law parameters, with

$$\vec{E}_{\mathrm{MC},y} = \sum_{x=1}^{q} \frac{1}{3} \rho L_x k_x Q_{xy}^{(m_x+1)} \quad \text{where } \vec{E}_{\mathrm{MC}} \in \mathbb{R}^p. \tag{44}$$

In this case, the statistical distribution of the randomly assigned parameters k_x and m_x, when considered collectively, aligns to an interpretation of the global statistical distribution (Fig. 6).

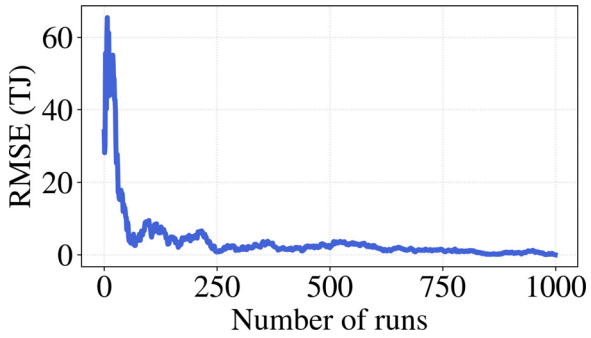

FIG. 7. Root mean square error (RMSE) of the Monte Carlo method after each run.

Applying the Monte Carlo method, n multiples of this vector can be produced and appended together to form a matrix $\mathbf{E}_{MC} \in \mathbb{R}^{p \times n}$. A vector $\bar{\vec{E}}_{MC}$ representing the mean of these runs is given by

$$\bar{\vec{E}}_{MC,y} = \frac{1}{n}\sum_{z=1}^{n} E_{MC,yz} \quad \text{where } \bar{\vec{E}}_{MC} \in \mathbb{R}^{p}. \tag{45}$$

The mean of this vector $\bar{\bar{E}}_{MC}$ represents the mean energy of all river reaches over this period, achieved with the Monte Carlo method, which can be summarized by

$$\bar{\bar{E}}_{MC} = \frac{1}{n}\sum_{z=1}^{n}\frac{1}{p}\sum_{y=1}^{p}\sum_{x=1}^{q}\frac{1}{3}\rho L_x k_{xz} Q_{xy}^{(m_{xz}+1)} \quad \text{where } \bar{\bar{E}}_{MC} \in \mathbb{R}. \tag{46}$$

III. RESULTS

A. Global theoretical riverine hydrokinetic resource

We estimate the global theoretical riverine hydrokinetic resource by calculating the total kinetic energy in the rivers of the world, excluding Greenland and Antarctica, over a 35 year period. Time series representing daily estimates of hydrokinetic energy in all river reaches, during the years 1979–2013, are created in two ways (Fig. 8). The first approach ($\bar{\vec{E}}_{MP}$) uses the mean values for power law parameters, as proposed by Moody and Troutman,[20] that are considered globally applicable (Fig. 6) to estimate the relevant hydraulic parameters required to quantify the kinetic energy flowing through a given river reach. The second approach ($\bar{\bar{E}}_{MC}$) uses a Monte Carlo method that randomly assigns power law parameters across all river reaches according to an inference of their statistical distribution. The former approach results in an estimate of $\bar{E}_{MP} = 2.315 \pm 0.004$ PJ [Eq. (43)], and the latter, the mean of the averages of $n = 1000$ runs, gives $\bar{\bar{E}}_{MC} = 5.911 \pm 0.009$ PJ [Eq. (46)]. Alternatively, these could be expressed as $\bar{E}_{MP} = 0.643 \pm 0.001$ TWh and $\bar{\bar{E}}_{MC} = 1.642 \pm 0.003$ TWh. In each case, the uncertainty of these estimates is a calculation of the standard error of the mean, applied to each time series. The Monte Carlo method has been applied to address the asymmetrical statistical distribution of these parameters. We argue that this asymmetry leads to a marked underestimate, as illustrated in Fig. 8, and represented by the first approach ($\bar{\vec{E}}_{MP}$), where global mean values for the power law parameters k and m were applied. For this reason, we consider the second approach ($\bar{\bar{E}}_{MC}$) as a more accurate representation of the global resource. In plotting the time series from both approaches, in addition to the mean values presented above, we illustrate the magnitude of the underestimate if uncertainties associated with the power law parameters are disregarded.

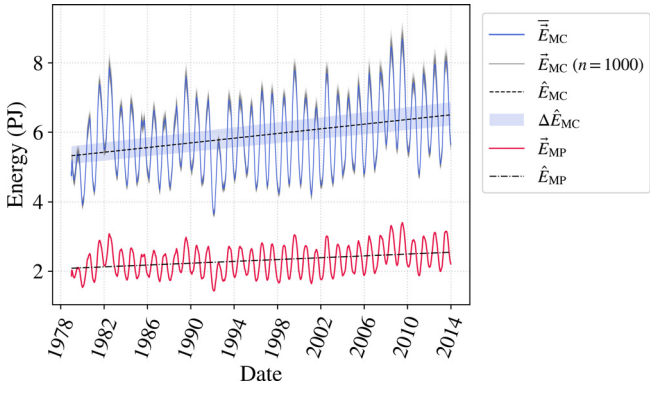

FIG. 8. Total daily energy of global rivers (excluding Greenland and Antarctica) between 1979 and 2013, with $\bar{\vec{E}}_{MP}$ calculated using mean values for power law parameters and $\bar{\vec{E}}_{MC}$ representing the mean of $n = 1000$ Monte Carlo simulations, where, in each case, $\vec{E}_{MC}$ is calculated with randomized power law parameters and applied to all reaches, such that the statistical distribution aligns with the assumed global statistical distribution. $\hat{E}_{MP}$ and $\hat{E}_{MC}$ provide a least squares fit in each case, and $\Delta\hat{E}_{MC}$ indicates the uncertainty as described by the range of values calculated by the Monte Carlo method.

It is typical to express an energy resource with units of TWh yr^{-1}, or similar, describing the average annual energy yield. Since this is a measure of energy conversion over a given time, it is a measure of power and actually an expression of the mean annual power. With a global theoretical riverine hydrokinetic resource assessment, we are considering the resource provided by the continuous movement of water through a global network of rivers. This could be regarded as analogous to a flywheel, which is often used to store energy, for example, in an automobile engine. Though the energy transfer through any cross section of this flywheel can be determined, providing a measure of power from a Eulerian perspective, the power of the flywheel as a whole is not possible to quantify. The flywheel has rotational energy, and any measure of power would depend upon the rate of extraction.

A clear rising trend (92 ± 46 GJd^{-1}) in inter-annual energy ($\hat{E}_{MC}$) is estimated (Fig. 8). The method applied in calculating energy is a function of Q, and therefore, any trends or fluctuations are due to changes in this variable. Reasons for this may be attributed to changes in factors such as precipitation or the rate of snow- and ice-melt. Though snow- and ice-melt do not appear to be directly input to the VIC model, used within GRADES, the later calibration steps include the use of a large number of empirical gauge measurements, which would certainly include the signal of any increase in Q due to these factors. Adler *et al.*[54] have considered global precipitation over a period (1979–2014), which coincides almost exactly with GRADES. Though they report an increase in atmospheric water vapor, coinciding with increased surface temperature, they find no overall significant trend for global precipitation. However, they do recognize regional patterns of positive and negative trends across the planet, with increases over tropical oceans and decreases over some middle latitude regions. An inter-annual trend may be attributed to longer-term changes in these factors, implying a change in the global climate. The rate of snow- and ice-melt would be expected to correlate with a rise in global temperature.[55] Rising global temperature has been linked to an increase in the intensity of the hydrological cycle,[56] but Held and Soden[57] advise against a simple assumption that global systems become more energetic as they warm, concluding that the complexity of such systems should guard against over-confidence in simple arguments.

An intra-annual oscillation ($\bar{\vec{E}}_{MC}$) is also seen in the time series, representing daily estimates of hydrokinetic energy (Fig. 8). This can be explained by natural seasonal variations in precipitation and the rates of snow- and ice-melt. A representation of an average year is achieved by calculating the mean energy on each calendar day (omitting leap days) throughout the 35 years considered [Fig. 9(a)]. Globally, a minimum of 4.8 ± 0.2 PJ occurs on 30 January and a maximum of 7.1 ± 0.4 PJ occurs on 23 July, corresponding with the

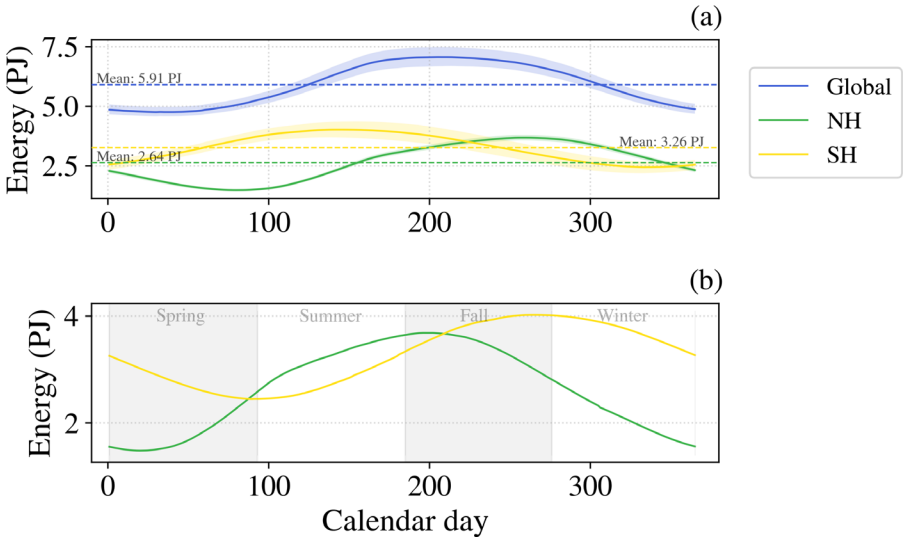

FIG. 9. Average year of daily energy for rivers globally, in the Northern Hemisphere (NH) and Southern Hemisphere (NH). The uncertainty of $n = 1000$ Monte Carlo simulations is indicated by the shaded area in (a) with calendar days from 1 January and (b) from the beginning of spring (1 March for the NH and 1 September for the SH).

Northern Hemisphere (NH) winters and summers, respectively (Table I summarizes all values associated with Fig. 9). The stated uncertainty of these estimates results from the extremes of the Monte Carlo simulations. The Monte Carlo method ($n = 1000$) is also applied to subsets of the data to determine the relative contributions from the NH and Southern Hemisphere (SH). Total river length (and percentage of global rivers, excluding Greenland and Antarctica) for the NH is 2.05×10^7 km (74.2%) and for the SH is 6.9×10^6 km (25.8%). Given this large difference in total river length between the two hemispheres, it is notable that the SH contributes a greater proportion to the global total. It is useful to also compare how hydrokinetic energy varies through the respective seasons of the two hemispheres [Fig. 9(b)]. Here, the numbering of the calendar days begins on the first day of spring, for each hemisphere, according to the meteorological definition (1 March and 1 September). The minimum and maximum in the NH are seen to occur at the beginning of spring and beginning of fall. For the SH, these occur at the end of spring and end of fall, illustrating a phase difference of approximately a season.

TABLE I. Complimentary data, corresponding with Figs. 9 and 10, stating mean, minimum, and maximum values: globally, by hemisphere, by continental-level basin, and hemisphere subdivisions of basins that straddle the equator. Calendar day and date of when minima and maxima occur are also given. The uncertainty stated with mean values is a calculation of the standard error of the mean, applied to the time series. Other uncertainties result from the extremes of the Monte Carlo simulations.

	Hydrokinetic energy (TJ)				Day		Date	
Basin	Mean	Min	Max	Range	Min	Max	Min	Max
Global	5911 ± 9	4800 ± 200	7100 ± 400	2300 ± 600	30	204	30 Jan	23 Jul
NH	2645 ± 7	1490 ± 60	3690 ± 80	2200 ± 140	80	260	21 Mar	17 Sep
SH	3266 ± 7	2500 ± 300	4000 ± 300	1500 ± 600	334	145	30 Nov	25 May
Africa	1103 ± 2	910 ± 60	1330 ± 100	420 ± 160	181	365	30 Jun	31 Dec
Europe	207.0 ± 0.4	150 ± 10	270 ± 10	120 ± 20	75	152	16 Mar	1 Jun
Siberia	460 ± 1	220 ± 20	620 ± 30	400 ± 50	103	265	13 Apr	22 Sep
Asia	771 ± 4	250 ± 10	1450 ± 70	1200 ± 80	80	261	21 Mar	18 Sep
Australia	96.3 ± 0.3	57 ± 4	135 ± 9	78 ± 13	230	98	18 Aug	8 Apr
S. America	2,873 ± 7	1900 ± 100	3800 ± 300	1900 ± 400	362	172	28 Dec	21 Jun
N. America	302 ± 1	190 ± 20	510 ± 60	320 ± 80	331	154	27 Nov	3 Jun
Arctic	103.1 ± 0.3	44 ± 5	143 ± 10	99 ± 15	103	267	13 Apr	24 Sep
Africa (NH)	543 ± 1	360 ± 30	750 ± 40	390 ± 70	84	303	25 Mar	30 Oct
Africa (SH)	562 ± 2	390 ± 50	830 ± 100	440 ± 150	199	34	18 Jul	3 Feb
Australia (NH)	24.52 ± 0.9	15 ± 2	33 ± 3	18 ± 5	229	15	17 Aug	15 Jan
Australia (SH)	71.9 ± 0.3	42 ± 3	110 ± 7	68 ± 10	234	98	22 Aug	8 Apr
S. America (NH)	231.8 ± 0.9	97 ± 8	376 ± 32	279 ± 40	89	225	30 Mar	13 Aug
S. America (SH)	2634 ± 7	1700 ± 200	3500 ± 300	1800 ± 500	357	162	23 Dec	11 Jun

With regard to this observed phase difference, Dettinger and Diaz[58] describe dominant modes of stream flow seasonality, which can be used to explain the maximum observed for the NH: a late spring stream flow maximum across the Timansky and Ural mountain ranges of Russia, along the southern edge of the Siberia, and in parts of the mountainous southwestern North America; the effects of a mid- to late-summer monsoon in the Indian subcontinent, eastern Africa, and Sahelian western Africa; and a slightly later (September) monsoon affecting tropical West Africa, Central America, and the subtropics of western North America. The SH signal is dominated by South America, which we shall discuss below, when comparing and contrasting individual continental basins.

Weather can be described as a manifestation of solar energy, which varies through the seasons due to the periodic oscillations of variables related to the earth's orbit of the sun and relative tilt of its axis. Precipitation and the rate of snow- and ice-melt are, thus, influenced by the effects of this process, dictating the observed seasonal variation of hydrokinetic energy. Beyond this, macroscopic weather events that would be most relevant in understanding seasonal variation in these factors are the occurrence of monsoons and the freezing and thawing of water at high elevation and high latitude.[59] The NH has substantially more landmass located at high latitude (Fig. 3) and is where many of the world's largest mountain ranges are found, although South America contains the Andes. Therefore, this would imply a greater effect from freezing and thawing in the NH, providing a plausible reason for the especially low minimum for the NH. Furthermore, it offers a valid hypothesis for the disproportionately greater hydrokinetic energy of the SH, overall, despite having markedly less total river length relative to the NH.

Verdin and Verdin[35] developed the Pfafstetter system to delineate and code hierarchically nested catchments. The GRADES dataset is divided into nine continental-level divisions, which are defined as Level 1 basins (Fig. 3). These nine continental-level divisions do not align to the conventional definition of the seven continents, with the exception of Africa and South America. This division allows investigation of the contribution to the global hydrokinetic resource by these regions [Fig. 10(a)]. South America is notable, with a mean of 2.870 ± 0.007 PJ (797 ± 0.002 GWh) accounting for 48.6% of the global mean (Table I summarizes all values associated with Fig. 10). Furthermore, a minimum and maximum occurring on 28 December and 21 June, both approximately a month prior to the global values, confirm the dominant signal of this continental-level basin.

The continental-level basins of Africa and Asia, with mean values of 1.103 ± 0.002 PJ (306.4 ± 0.6 GWh) and 0.771 ± 0.004 PJ (214 ± 1 GWh), are the next greatest. Though the continental-level basins of South America and Africa align with the contemporary definitions of these continents, that is not the case for Asia. For a thorough quantification of the Asian continent, a consideration of portions of the continental-level basins of Siberia and Australia would be needed and surely result in the energy attributed to this continent increasing. Therefore, the results of this resource assessment would suggest that the continents of South America, Africa, and Asia are those that offer the most potential, in terms of HEC.

The Siberia and Arctic continental-level basins, though containing major rivers (e.g., Mackenzie, Yukon, Kolyma, Lena, Khatanga, Yenisey, and Ob), contribute modestly to the global total, with mean values of 0.460 ± 0.001 PJ (127.8 ± 0.03 GWh) and 103.1 ± 0.3TJ (28.64 ± 0.08 GWh), respectively. The low values for these regions of higher latitudes would suggest that the contributions from Greenland and Antarctica, which are not part of this study, would also be low. Both regions are similarly affected by the colder temperatures found at high latitude, causing much water to be held as ice and snow, and neither region contains any notably large rivers. Furthermore, high latitudes are associated with reduced precipitation.[60,61] These factors reinforce the assertion that higher latitude, less hydrokinetic energy abundant, and areas of the NH result in the disproportionately high estimation for the hydrokinetic energy for the SH, with respect to the latter having less total river length.

The continental-level basins of Africa, Australia, and South America straddle the equator, with each having 30%, 92%, and 83% of their total river length located in the SH and the remainder in the NH. Therefore, consideration of the average annual years for these basins, plotted with calendar days beginning from a hemisphere-specific start of spring (1 March and 1 September), required dividing the data into

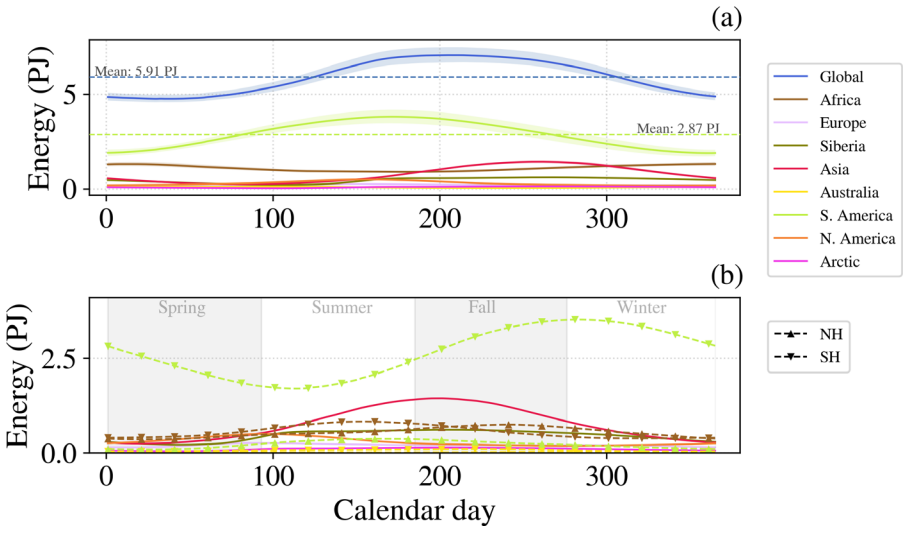

FIG. 10. Average year of daily energy for rivers globally and by continental-level division. The uncertainty of $n = 1000$ Monte Carlo simulations is indicated by the shaded area in (a) with calendar days from 1 January and (b) from the beginning of spring (1 March for the NH and 1 September for the SH). Continental-level divisions represented in the NH and SH are appropriately divided.

further subsets [Fig. 10(b)]. The strongest signals for the NH and SH, respectively, are the continental-level basins of Asia and the SH subset of South America (Table I). The continental-level basin of Asia has a minimum occurring on the same day as for the overall NH subset and a maximum that occurs a day later. This basin contains a number of major rivers that transport water from the Himalayas and is governed by strong precipitation seasonality, with up to 80% of the annual rainfall occurring during the Indian summer monsoon season.[62] Though the Indian summer monsoon exhibits a wide spectrum of variability, the season is generally from June to September,[62,63] describing the meteorological definition of the NH summer. This monsoon and the East Asian monsoon are the major components of the larger Asian monsoon system.[63] The East Asian summer monsoon also contributes significant precipitation during the NH summer, with two peaks from late June to mid-July and from mid-August to early September.[64] These high precipitation events occur during a corresponding rise in the estimated hydrokinetic energy for this basin, following the initiation of the rise from probable ice- and snow-melt at the beginning of the spring, marked by the minimum on 21 March and maximum on 18 September (40 and 201 days after the beginning of spring).

The SH subset of the South America continental-level basin is seen to lead Asia (and the NH as a whole, as discussed above) by approximately a season, with a rise beginning from a minimum on 23 December and maximum on 11 June (113 and 283 days after the beginning of spring). Zhou and Lau[65] first confirmed that a monsoon climate exists over South America and describe the South American summer monsoon as a complex and multi-phase process, involving much regional variation. This can be summarized, more generally, as involving increased precipitation on the continent from late spring to late summer. This period correlates with the maximum gradient of increased hydrokinetic energy, before a gradual reduction, reaching a maximum at the end of the fall. Since the effects of monsoons occur in approximately the same seasons, for the Asia basin and SH subset of the South America basin, the lag of a season between the former and the latter must be due to another factor. Transmission time, which describes how long it takes for rainfall to flow through a catchment, is inevitably important here and provides some explanation for the observed lag of maximum hydrokinetic energy behind expected maximum rainfall. Yet, this would be the case for both the Asia and the SH subset of the South America continental-level basins and does, therefore, not explain the difference in the length of the lag between them. Given the heavy influence of the Himalayas on the rivers of the Asia basin, and the fact that it is the most significant and highest mountain range on Earth, it might be the case that the freezing and thawing process, which affects the volume of water available to contribute to the overall discharge, is relevant. Indeed, Bookhagen and Burbank[62] provide a detailed description of the spatiotemporal variability of the Indian summer monsoon in the Himalayas and highlight the importance of ice- and snow-melt in the hydrological budget of Himalayan rivers. The authors state that this is particularly significant in the pre- and early monsoon months from March to June, accounting for >40% of river discharge.

B. Global distribution of riverine hydrokinetic resource

The spatial distribution of the riverine hydrokinetic resource is determined by river reach, using an equation derived from a consideration of the rate of transfer of kinetic energy (Eq. (37)). It is increasingly common for hydrological studies to use a reach-scale frame of reference.[24,66,67] A reach is a length of a river, between points of confluence, bifurcation, or channel initiation. It usually suggests a level, uninterrupted stretch. This definition allows hydrological characteristics to be considered at an intermediate scale, between catchment- and field-scale. The growth of "big data" in geosciences allows higher fidelity data than can be achieved at the catchment-scale. Yet, a better understanding can be achieved at the reach-scale than for field-scale, as the numerous assumptions and approaches used in hydrological modeling still work reasonably well at this scale.

Hydrokinetic power predominately resides in major rivers, increasing in the downstream direction (Fig. 11). River reaches are shown with linewidth proportional to stream order. Stream order provides a means for describing a river system as a network, with nodes and links.[68] Consider the river network of the Amazon (Fig. 12). It can be seen that stream order gives some indication of the reaches that are contained in larger river networks and their position within these river

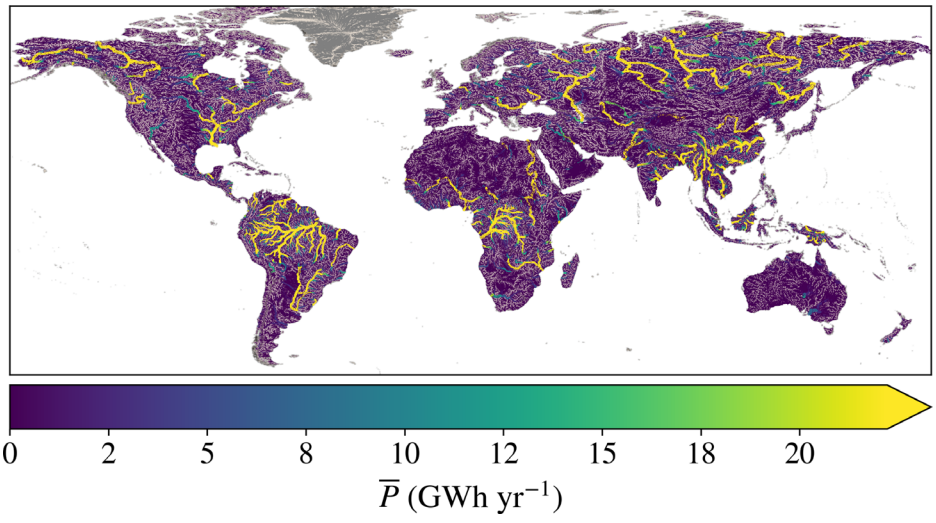

FIG. 11. Global (excluding Greenland and Antarctica) spatial distribution of theoretical riverine hydrokinetic mean annual power $\overline{P}$. Lines representing rivers have a width that is proportional to stream order. The colorbar maximum is determined by the 99th percentile.

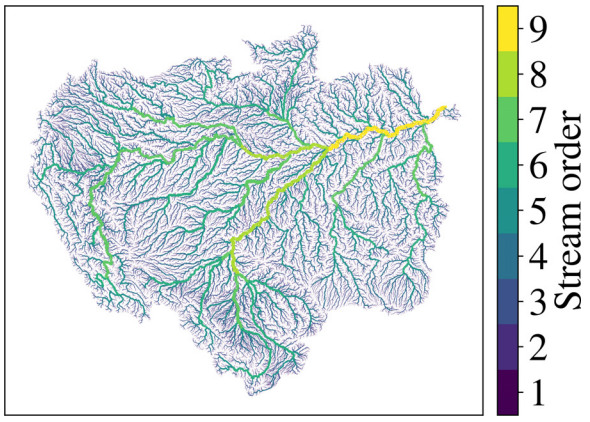

FIG. 12. Stream order values in the Amazon river network.

networks. The river is shown developing in a downstream direction and illustrates that the lower-courses of large river system are assigned a high value for stream order, with the final reaches having the maximum values. In contrast, smaller river networks reach the sea at lower stream orders. Thus, stream order on a global scale gives an overall measurement of both river network size and distance downstream. Stream order numbers are assigned to each node, in bottom-up order, according to the following criteria: if the node is a leaf (has no children), its number is 1; if the node has one child with number i and all other children have numbers less than i, then the number of the node is i again; and, if the node has two or more children with number i and no children with greater number, then the number of the node is $i+1$. Each river reached in the GRADES dataset used in this study has been assigned a number from 1 to 9.

Since larger rivers will tend to contain reaches with higher steam orders, the preponderance of hydrokinetic power in larger rivers is confirmed by the apparent concentration of power in rivers that have been plotted with thicker lines [Fig. 15(a)]. Plotting hydrokinetic power against stream order confirms that this is, indeed, the case (Fig. 13).

Having been identified as containing the highest estimated hydrokinetic resource (Fig. 10), it is instructive to isolate the South America continental-level basin (Fig. 14). Here, a number of major rivers can be identified, including the Amazon, Orinoco, Río de la Plata, Tocantins, Magdalena, São Francisco, and their tributaries. This identification is achieved as a result of the colors in this choropleth plot, which, in addition to tracing out these rivers, also demonstrates their considerable hydrokinetic power. Furthermore, the thicker lines that are discernible in these larger river networks illustrate the distribution of stream order values and confirm the increase in hydrokinetic power in a downstream direction.

Leopold and Maddock[19] established a method for estimating hydraulic parameters as a function of Q [Eqs. (23)–(25)]. Estimated global mean values for the power law parameters k and m were used to calculate mean hydrokinetic power. Although consideration of a single reach is best represented, statistically, by these mean values, when considered collectively, this results in a marked underestimation. In publishing globally applicable numerical constants for the coefficients and exponents of power law relationships to estimate the hydraulic parameters mean width and depth, Moody and Troutman[20] provided an indication of the 95% confidence intervals associated with the coefficients of these relationships. These confidence intervals are asymmetric about the mean values (Fig. 6), being notably larger in the positive direction. We have used these published values to derive corresponding values for k, m, and their associated uncertainty [Eq. (41)]. Therefore, this asymmetry also exists for the 95% confidence interval for the coefficient k. Given that confidence intervals would reflect the statistical distribution of these parameters, this asymmetry implies empirical values of annual mean power that, though they can be calculated using power law coefficients falling within this confidence interval, are of a magnitude that greatly exceeds that predicted by an estimation using an application of the mean values. Conversely, empirical values of annual mean power, which can also be calculated using power law coefficients that fall within the confidence interval, but of a

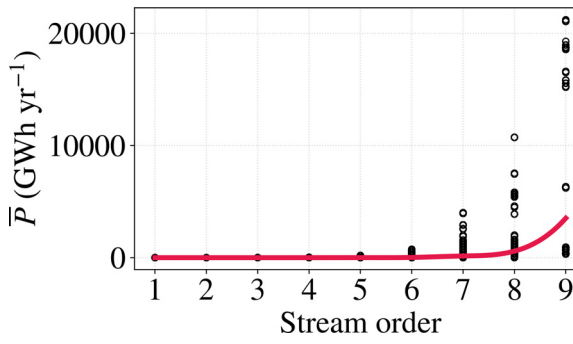

FIG. 13. Hydrokinetic annual mean power $\bar{P}$ of all reaches, globally, plotted against stream order.

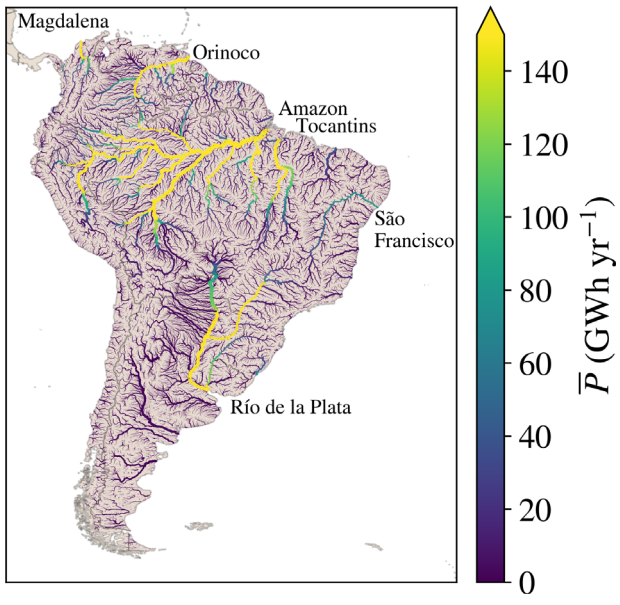

FIG. 14. Spatial distribution of hydrokinetic annual mean power $\bar{P}$ within the South American continental-level basin. Prominent rivers of the region are labeled.

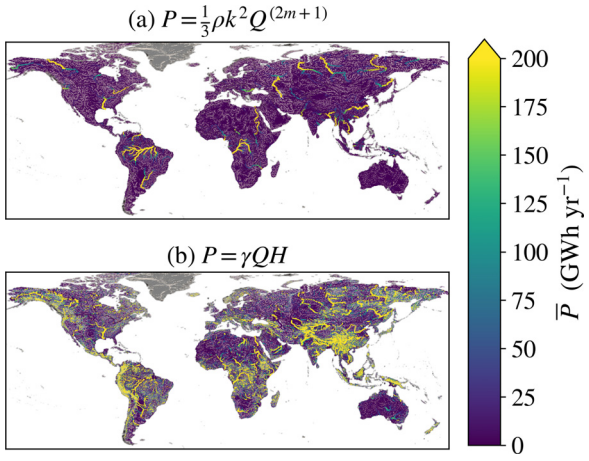

FIG. 15. Global (excluding Greenland and Antarctica) spatial distribution of theoretical riverine hydrokinetic annual mean power $\bar{P}$, using an equation derived from a perspective of (a) the transfer of kinetic energy and (b) the conversion from gravitational potential energy. The colorbar maximum is set "by eye," to best compare and contrast the plots.

magnitude that is below that estimated using an application of mean values, would tend to have a lesser magnitude of variance, overall.

C. Comparison with existing studies

An earlier study,[16] using the same GRADES data applied here, provides a global perspective for comparison [Fig. 15(b)]. Both this earlier study and what we present here use a similar approach, with the earlier study applying the conventional equation $P = \gamma QH$ [Eq. (1)], providing a measurement of the theoretical rate of conversion of gravitational potential energy to kinetic energy. In contrast, the equation $P = \frac{1}{3}\rho k^2 Q^{(2m+1)}$ [Eq. (37)] as applied in this study provides a measurement of the theoretical rate of transfer of kinetic energy through river systems.

Comparison of these two sets of results reveals distinct differences. A qualitative description of regions that are prominent, from the perspective of the earlier study, would include: the Himalayas, Tibetan Plateau, and surrounding areas; the large, mountainous islands of Borneo, Indonesia, and New Guinea; New Zealand; the Andes; the Pacific Northwest; Scandinavia; the Congo Basin and Equatorial Africa; Madagascar; and many of the major rivers of the world [Fig. 15(b)]. Or, more succinctly: regions with large changes in elevation and many major rivers. This contrasts with the revised methodology applied in this study, which highlights that the resource resides predominately in the major rivers of the world, with the resource increasing in the downstream direction (Fig. 15(a)). In addition to the qualitative differences described, overall estimates of the annual mean power also tend to be notably lower in the hydrokinetic approach applied in this study.

A relative assessment of this difference (Fig. 16) is considered by subtracting the normalized hydrostatic annual mean power from the normalized hydrokinetic annual mean power. The calculation of this normalized difference in power $\bar{P}_{\text{diff}}$, for each reach, can be summarized as

$$\bar{P}_{\text{diff}} = \frac{\bar{P}_{\text{GPE}}}{\bar{P}_{\text{GPE,99}}} - \frac{\bar{P}_{\text{KE}}}{\bar{P}_{\text{KE,99}}}, \tag{47}$$

where $\bar{P}_{\text{GPE}}$ is the mean annual power of a reach from a gravitational potential energy derived (hydrostatic) perspective [Eq. (1)], $\bar{P}_{\text{KE}}$ is the mean annual power of a reach from a kinetic energy derived (hydrokinetic) perspective [Eq. (37)], and the associated global 99th percentile values are $\bar{P}_{\text{GPE,99}}$ and $\bar{P}_{\text{KE,99}}$. The hydrostatic resource assessment is seen to favor areas with large elevation change, whereas the hydrokinetic resource assessment favors major rivers, thus confirming the interpretation of Fig. 15 stated above. In the former, the conventional equation for determining theoretical hydraulic power ($P = \gamma QH$) is used, which is derived from considering the rate of conversion of gravitational potential energy to kinetic energy that occurs as water travels along the length of a river reach (see Subsection I A). In the latter, an equation is proposed ($P = \frac{1}{3}\rho k^2 Q^{(2m+1)}$) that considers the rate of transfer of energy that propagates through any cross section within a given river reach and involves estimating the mean width, depth, and flow velocity of this reach, as a function of the mean discharge (see Subsection II B). Power, conceptually, is defined as either the rate of

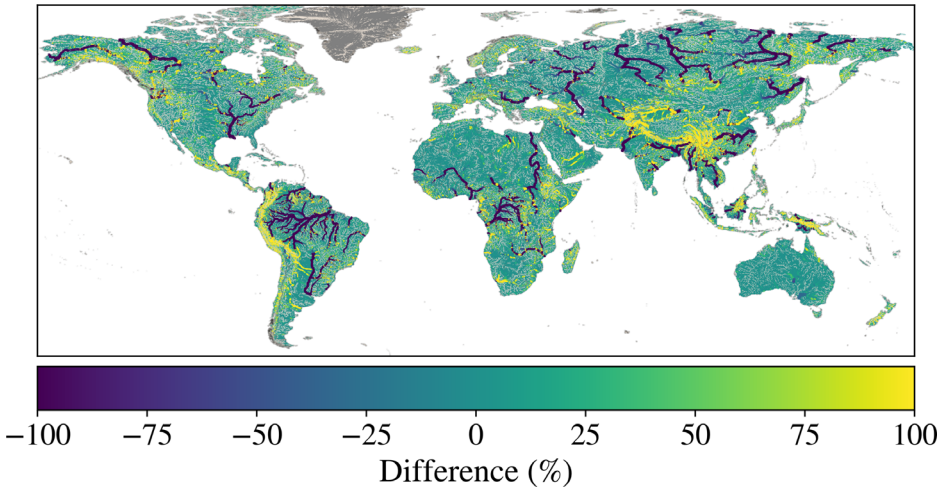

FIG. 16. The difference between resource assessment from a hydrokinetic and hydrostatic approach, where 0% implies no difference between the normalized values from each, 100% a maximum difference biased toward the hydrostatic calculation, and −100% a maximum difference toward the hydrokinetic calculation. Line width is proportional to stream order.

energy conversion or the rate of energy transfer. The two perspectives (hydrostatic and hydrokinetic) align with these two definitions, respectively. In stating this, we more precisely determine what is being measured by these two approaches and make clear what might be expected to result from assessing the global hydrokinetic resource through these two lenses. We find that these two methods provide different results and disagree on a qualitative and quantitative description of the regions of the world that have the most potential for HEC.

The two approaches differ in their frame of reference and, therefore, offer slightly different ways of viewing the resource. The hydrostatic perspective uses a Lagrangian frame of reference, giving an estimate of the kinetic energy of the water flowing through only the final cross section of a river reach. In contrast, the hydrokinetic perspective is Eulerian and considers the rate of transfer of energy that is transferred through a given cross section. Since hydraulic geometry parameters are considered constant along reaches, in this study, the hydrokinetic energy approach is applicable to any cross section within a reach, including the final cross section. This point, concerning the final cross sections, is the reason why the two methods can be compared and contrasted. In describing a Lagrangian frame of reference, we are considering a discrete body of water moving through space and time. This can be extended to a global view, where the river network comprises many individual discrete bodies of water and is defined by the sum of these individual reaches. In this way, a global resource assessment is achieved by considering a "snapshot," where the flow of each of these discrete bodies is considered flowing through each of these reaches. Though the period in which this occurs for each reach will differ, this is not important, since the sum of these discrete bodies of water equals the sum of all water in the global network. In the derivation of the equation used for the hydrokinetic approach, we described a body of water traveling a given length in a given time (see Subsection II B). This leads to a complication when considering all global reaches concurrently, since the time will vary for each reach, if considering a discretized body of water traveling through these reaches. To put this another way, if two reaches with the same value for discharge but different lengths are considered, they will have the same calculation of power but will transfer a different quantity of energy when considered over the same time period. Alternatively, a different period of time will elapse if considering the transfer of these discrete quantities of water. This inconsistency is another reason that a value for the global theoretical riverine resource as an expression of annual energy yield, using the usual units of TWh yr^{-1} or similar, is not offered in this study. The means for achieving an estimate of the mean total energy of all rivers as 5.911 ± 0.009 PJ (1.642 ± 0.003 TWh), as presented in Subsection III A, involved discretizing the water contained within each reach and are, therefore, now Lagrangian in nature, in contrast to the Eulerian method of measuring power transferred through the reach. Though operating within different frames of reference, both still offer a hydrokinetic perspective.

Studies providing accurate measurements of the theoretical hydrokinetic resource in rivers are few. Punys *et al.*[1] used the one-dimensional hydraulic model HEC RAS 4.1 to determine the theoretical hydrokinetic power passing through cross sections at three locations in Lithuania. The determination of the coordinates of these locations (P. Punys and E. Kasiulis,[1] Pers. Comm.) allowed identification of the corresponding river reaches, such that a comparison could be made between the two methods considered here (Table II).

TABLE II. Comparison of annual mean power ($\bar{P}_{mod}$), as calculated by Punys *et al.*,[1] with that calculated using a hydrostatic method ($P_{GPE} = \gamma QH$) and a hydrokinetic method ($P_{KE} = \frac{1}{3}\rho k^2 Q^{(2m+1)}$).

Location	$\bar{P}_{mod}$ (kW)	$\bar{P}_{GPE}$ (kW)	$\bar{P}_{KE}$ (kW)
Jonava	124	1165	153
Vilnius	52	14 307	83
Buivydziai	24	6612	52

The values for annual mean power calculated using the hydrostatic approach ($\bar{P}_{GPE}$) for the locations Jonava, Vilnius, and Buivydziai differ from the hydraulic model calculations ($\bar{P}_{mod}$) by 840%, 27 413%, and 27 450%, respectively. The hydrokinetic approach ($\bar{P}_{KE}$), using mean values $m = 0.5$ and $k = 0.20$, yielded values that differed by 23%, 60%, and 117%, respectively. Percentage bias (PBIAS) measures the average tendency of simulated values S to be larger or smaller than observed values O, using

$$\mathrm{PBIAS} = \frac{\sum_{i=1}^{N}(S_i - O_i)}{\sum_{i=1}^{N} O_i} \times 100\%, \tag{48}$$

with an optimal value of PBIAS = 0% and low-magnitude values, indicating accurate model simulation. Positive and negative values signify over- and under-estimation bias, respectively. If we treat the calculations from these two studies as simulated values and the data from Punys *et al.*[1] as observed values, the PBIAS for the hydrostatic and hydrokinetic approach is $+11\,000 \pm 5435\%$ and $+40^{+7.994}_{-139}\%$, respectively. The uncertainty in the former case is a measure of the mean absolute error. In the latter case, addressing the more prominent source of uncertainty, this is determined by using the upper and lower limits for the 95% confidence interval and uncertainty of the power law parameters m and k, respectively, giving an uncertainty that is asymmetric with respect to the mean values [Eq. (41)]. While this is a small sample size to provide a complete validation and there are large uncertainties associated with the parameters m and k used to calculate the mean power from the hydrokinetic perspective ($\bar{P}_{KE}$), this comparison would suggest that the hydrokinetic method for estimating hydrokinetic resource provides a result that agrees more closely to the results from the hydraulic model applied by Punys *et al.*[1] We reiterate that the sample size is small, yet observe that considerable differences are seen between these two approaches; sufficient, perhaps, to conclude that this is a meaningful difference.

IV. DISCUSSION

Since hydrokinetic power is proportional to flow velocity cubed [Eq. (22)], it follows that flow velocity is of fundamental importance to a meaningful resource assessment. Leopold and Maddock[19] have demonstrated that flow velocity is proportional to discharge [Eq. (25)]. Major rivers have high values for discharge, and this would tend to increase in a downstream direction, reinforcing our finding that downstream regions contain the greatest potential for HEC. An increase in

flow velocity in a downstream direction also accords with the Bradshaw model of upper- to lower-river course trends.[22,23]

A dynamic equilibrium between tectonic uplift, tectonic deformation, and geomorphic processes of erosion, modulated by geology, substrate erodability, and climate, drives the evolution of a river network. The resulting geometry is that which serves the role of draining a terrestrial landscape of water and sediment most efficiently. Constructal theory describes a law of design and evolution in nature and states that finite-size flow systems must evolve to provide increasing access to the currents that flow through them.[69] Examples are seen in the evolution of lungs, animal locomotion, vegetation, turbulent flow structure, self-lubrication, natural multi-scale porous media, and also river basins.[70] This law has been suggested not only for temporal evolution but also in a downstream direction[71] and implies an increase in efficiency and, therefore, increase in energy. Such a perspective would align with a view that the lower-courses of major rivers would potentially offer river flow with the greatest kinetic energy, corresponding to the hydrokinetic focused methodology and associated results presented here.

We argue that a methodology that focuses on flow velocity and the rate of transfer of kinetic energy, in considering the global theoretical riverine hydrokinetic resource, rather than an unrealistic measurement of the rate of conversion of gravitational potential energy to kinetic energy, better supports the development of HEC technology, in an immature industry where such information has been identified as one of the main barriers to progress.[2,11] A hydrostatic perspective of this resource is still relevant and permits an estimation of the overall annual mean energy yield, which can be compared with other renewable energy technologies. Yet, it must be realized that this hydrostatic approach is theoretical and discounts energy loss due to boundary-induced friction. This issue is compounded by the fact that friction from the bed and banks of a channel is not constant throughout a river network, from upper- to lower-courses, resulting in a bias when used as a means for determining global distribution (see Subsection I A).

Large uncertainties are associated with the power law parameters used in the hydrokinetic approach we present. This could be summarized as giving a method that is less precise, relative to the conventional hydrostatic perspective, but arguably more accurate. Future studies could look to improve this precision. The development of techniques for estimating continental- and global-scale river widths has shown steady improvement.[72–74] Since discharge is the product of the hydraulic parameters width, depth, and flow velocity [Eq. (32)], a corresponding improvement of techniques to determine depth, in combination with datasets for discharge, such as used in this study, would lead to a better estimate of flow velocity, which is probably the most challenging of these variables to determine remotely.

Given the focus upon flow velocity in the methodology and results we present, we must acknowledge and highlight the limitations of this approach, due to this fact, in addition to the benefits that we have laid out, thus, far. Attempting a global-scale resource assessment necessitates an acceptance of decreased resolution, with decreasing resolution comes ever-decreasing representation of the variability of flow velocity. At the reach-scale, the natural variability of the channel form results in corresponding effects upon flow velocity and an accompanying impact upon hydrokinetic energy. This reach-scale variability is not captured in our study. In their review of riverine hydrokinetic resource assessments, Kirby *et al.*[75] found that the methodology applied to site-specific assessments was not entirely consistent. Furthermore, they state that these issues are amplified for regional-scale, or larger-scale, resource assessments. Though the standards published by the International Electrotechnical Commission[76,77] propose a standardized approach to site-specific resource assessment, they provide no advice on how this site is first identified. This study looks to offer something in the way of a first-order approximation that can bridge this gap. Overall, we offer a general perspective to describe where hydrokinetic energy is to be found and make explicit the difference between conventional hydropower and HEC, and the need for different approaches to resource assessment for each.

V. CONCLUSION

We propose a method for theoretical riverine hydrokinetic resource assessment that focuses directly on kinetic energy, rather than the established method that relies upon the conversion from gravitational potential energy. Perspective of the global distribution of this resource is quite different with this new approach. Traditional use of the conventional equation for determining theoretical hydraulic power, which focuses on energy that can be harnessed from a hydrostatic approach, highlights regions of the world with large elevation change and major rivers. In contrast, an equation derived from kinetic energy provides a truly hydrokinetic approach. In this case, major rivers, and particularly the lower-courses of major-rivers, are found to offer the most potential for hydrokinetic energy conversion. Large uncertainties are certainly inherent in this proposed methodology, but we argue that, though less precise, this offers a more accurate and pragmatically useful view. Advancements in remote sensing and developments of techniques for extracting more hydraulic geometry information from ever-increasing "big data" hint at future improvements in precision that can enhance this methodology.

ACKNOWLEDGMENTS

The authors acknowledge the funding support from the Knowledge Economy Skills Scholarships (KESS 2) and Repetitive Energy Company. KESS 2 is a pan-Wales higher level skills initiative led by the Bangor University on behalf of the HE sector in Wales. It is, in part, funded by the Welsh Government's European Social Fund (ESF) convergence programme for West Wales and the Valleys. We acknowledge the support of the Supercomputing Wales project, which is, in part, funded by the European Regional Development Fund (ERDF) via the Welsh Government. We also acknowledge the support of the Smart Efficient Energy Centre (SEEC) at Bangor University, partially funded by the European Regional Development Fund (ERDF), administered by the Welsh Government.

AUTHOR DECLARATIONS

Conflict of Interest

The authors have no conflicts to disclose.

Author Contributions

Michael Ridgill: Conceptualization (lead); Data curation (lead); Formal analysis (lead); Investigation (lead); Methodology (lead); Software (lead); Validation (lead); Writing – original draft (lead);

Writing – review and editing (lead). **Matt J Lewis:** Supervision (supporting); Writing – review and editing (supporting). **Peter E Robins:** Supervision (supporting); Writing – review and editing (supporting). **Sopan D Patil:** Writing – review and editing (supporting). **Simon Neill:** Project administration (lead); Supervision (lead); Writing – review and editing (supporting).

DATA AVAILABILITY

The data that support the findings of this study are available within the article.

REFERENCES

[1]P. Punys, I. Adamonyte, A. Kvaraciejus, E. Martinaitis, G. Vyciene, and E. Kasiulis, "Riverine hydrokinetic resource assessment. A case study of a lowland river in Lithuania," Renewable Sustainable Energy Rev. **50**, 643–652 (2015).

[2]M. Khan, M. Iqbal, and J. Quaicoe, "River current energy conversion systems: Progress, prospects and challenges," Renewable Sustainable Energy Rev. **12**, 2177–2193 (2008).

[3]IRENA, "Renewable capacity statistics 2019," Technical Report (International Renewable Energy Agency (IRENA), 2019).

[4]IEA, "Renewables information: Overview," Technical Report (Paris: IEA/OECD, 2020).

[5]P. Moriarty and D. Honnery, *Rise and Fall of the Carbon Civilisation: Resolving Global Environmental and Resource Problems* (Springer Science & Business Media, 2010).

[6]R. E. Sims, R. N. Schock, A. Adegbululgbe, J. Fenhann, I. Konstantinaviciute, W. Moomaw, H. B. Nimir, B. Schlamadinger, J. Torres-Martinez, C. Turner *et al.*, "Energy supply," in *Climate Change 2007: Mitigation. Contribution of Working Group III to the Fourth Assessment Report of the Intergovernmental Panel on Climate Change*, edited by B. Metz, O. R. Davidson, P. R. Bosch, R. Dave, and L. A. Meyer (Cambridge University Press, 2007), pp. 252–322.

[7]S. Abbasi and N. Abbasi, "The likely adverse environmental impacts of renewable energy sources," Appl. Energy **65**, 121–144 (2000).

[8]M. McCartney, "Living with dams: Managing the environmental impacts," Water Policy **11**, 121–139 (2009).

[9]D. Pimentel, M. Herz, M. Glickstein, M. Zimmerman, R. Allen, K. Becker, J. Evans, B. Hussain, R. Sarsfeld, A. Grosfeld *et al.*, "Renewable energy: Current and potential issues: Renewable energy technologies could, if developed and implemented, provide nearly 50% of US energy needs; this would require about 17% of US land resources," Bioscience **52**, 1111–1120 (2002).

[10]A. Ansar, B. Flyvbjerg, A. Budzier, and D. Lunn, "Should we build more large dams? The actual costs of hydropower megaproject development," Energy Policy **69**, 43–56 (2014).

[11]N. D. Laws and B. P. Epps, "Hydrokinetic energy conversion: Technology, research, and outlook," Renewable Sustainable Energy Rev. **57**, 1245–1259 (2016).

[12]UMA Group, "An evaluation of the kinetic energy of Canadian rivers & estuaries," Technical Report (Canadian National Research Council-Canadian Hydraulics Centre, 1980).

[13]G. Miller, J. Franceschi, W. Lese, and J. Rico, "The allocation of kinetic hydro energy conversion systems (KHECS) in USA drainage basins: Regional resource and potential power," Technical Report (US Department of Energy, 1986).

[14]R. Jenkinson and J. Bomhof, "Assessment of Canada's hydrokinetic power potential: Phase III report, resource estimation," Technical Report (National Research Council of Canada, 2014).

[15]P. T. Jacobson, T. M. Ravens, K. W. Cunningham, and G. Scott, "Assessment and mapping of the riverine hydrokinetic resource in the continental United States," Technical Report No. DOE/EE/0002662-1 (Electric Power Research Institute, 2012).

[16]M. Ridgill, S. P. Neill, M. J. Lewis, P. E. Robins, and S. D. Patil, "Global riverine theoretical hydrokinetic resource assessment," Renewable Energy **174**, 654–665 (2021).

[17]D. Knighton, *Fluvial Forms and Processes: A New Perspective* (Routledge, 2014).

[18]S. P. Neill and M. R. Hashemi, *Fundamentals of Ocean Renewable Energy* (Elsevier, 2018).

[19]L. B. Leopold and T. Maddock, "The hydraulic geometry of stream channels and some physiographic implications," U.S. Geol. Survey Professional Paper **252**, 481–492 (1953).

[20]J. A. Moody and B. M. Troutman, "Characterization of the spatial variability of channel morphology," Earth Surf. Processes Landforms **27**, 1251–1266 (2002).

[21]D. Bernoulli, *Hydrodynamica: Sive de Viribus et Motibus Fluidorum Commentarii* (Johannis Reinholdi Dulseckeri, 1738).

[22]M. J. Bradshaw, A. J. Abbott, and A. Gelsthorpe, *The Earth's Changing Surface* (John Wiley & Sons, 1978).

[23]S. A. Schumm, *The Fluvial System* (Wiley-Interscience Publications, New York, 1977).

[24]P. Lin, M. Pan, H. E. Beck, Y. Yang, D. Yamazaki, R. Frasson, C. H. David, M. Durand, T. M. Pavelsky, G. H. Allen *et al.*, "Global reconstruction of naturalized river flows at 2.94 million reaches," Water Resour. Res. **55**, 6499–6516, https://doi.org/10.1029/2019WR025287 (2019).

[25]X. Liang, D. P. Lettenmaier, E. F. Wood, and S. J. Burges, "A simple hydrologically based model of land surface water and energy fluxes for general circulation models," J. Geophys. Res. **99**, 14415–14428, https://doi.org/10.1029/94JD00483 (1994).

[26]J. J. Hamman, B. Nijssen, T. J. Bohn, D. R. Gergel, and Y. Mao, "The Variable Infiltration Capacity model version 5 (VIC-5): Infrastructure improvements for new applications and reproducibility," Geosci. Model Dev. **11**, 3481–3496 (2018).

[27]C. H. David, D. R. Maidment, G.-Y. Niu, Z.-L. Yang, F. Habets, and V. Eijkhout, "River network routing on the NHDPlus dataset," J. Hydrometeorol. **12**, 913–934 (2011).

[28]D. Yamazaki, D. Ikeshima, J. Sosa, P. D. Bates, G. Allen, and T. Pavelsky, "MERIT Hydro: A high-resolution global hydrography map based on latest topography datasets," Water Resour. Res. **55**, 5053–5073, https://doi.org/10.1029/2019WR024873 (2019).

[29]D. Yamazaki, D. Ikeshima, R. Tawatari, T. Yamaguchi, F. O'Loughlin, J. C. Neal, C. C. Sampson, S. Kanae, and P. D. Bates, "A high-accuracy map of global terrain elevations," Geophys. Res. Lett. **44**, 5844–5853, https://doi.org/10.1002/2017GL072874 (2017).

[30]D. Yamazaki, M. A. Trigg, and D. Ikeshima, "Development of a global 90 m water body map using multi-temporal Landsat images," Remote Sens. Environ. **171**, 337–351 (2015).

[31]J.-F. Pekel, A. Cottam, N. Gorelick, and A. S. Belward, "High-resolution mapping of global surface water and its long-term changes," Nature **540**, 418–422 (2016).

[32]B. Lehner, K. Verdin, and A. Jarvis, *HydroSHEDS Technical Documentation, Version 1.0* (World Wildlife Fund US, Washington, DC, 2006).

[33]H. Wu, J. S. Kimball, H. Li, M. Huang, L. R. Leung, and R. F. Adler, "A new global river network database for macroscale hydrologic modeling," Water Resour. Res. **48**, W09701, https://doi.org/10.1029/2012WR012313 (2012).

[34]D. G. Tarboton, "A new method for the determination of flow directions and upslope areas in grid digital elevation models," Water Resour. Res. **33**, 309–319, https://doi.org/10.1029/96WR03137 (1997).

[35]K. L. Verdin and J. P. Verdin, "A topological system for delineation and codification of the Earth's river basins," J. Hydrol. **218**, 1–12 (1999).

[36]R. E. Bell, A. F. Banwell, L. D. Trusel, and J. Kingslake, "Antarctic surface hydrology and impacts on ice-sheet mass balance," Nat. Clim. Change **8**, 1044–1052 (2018).

[37]G. H. Allen and T. M. Pavelsky, "Patterns of river width and surface area revealed by the satellite-derived North American river width dataset," Geophys. Res. Lett. **42**, 395–402, https://doi.org/10.1002/2014GL062764 (2015).

[38]C. C. Park, "World-wide variations in hydraulic geometry exponents of stream channels: An analysis and some observations," J. Hydrol. **33**, 133–146 (1977).

[39]R. E. Glover and Q. Florey, "Stable channel profiles," United States Bureau of Reclamation, Engineering Laboratories Branch, Hydraulic Laboratory Report No. HYD-325 (1951).

[40]F. M. Henderson, "Stability of alluvial channels," J. Hydraul. Div. **87**, 109–138 (1961).

[41]E. W. Lane, "Design of stable channels," Trans. Am. Soc. Civil Eng. **120**, 1234–1260 (1955).
[42]S. Biancamaria, K. M. Andreadis, M. Durand, E. A. Clark, E. Rodriguez, N. M. Mognard, D. E. Alsdorf, D. P. Lettenmaier, and Y. Oudin, "Preliminary characterization of SWOT hydrology error budget and global capabilities," IEEE J. Sel. Top. Appl. Earth Obs. Remote Sens. **3**, 6–19 (2009).
[43]K. M. Andreadis, G. J.-P. Schumann, and T. Pavelsky, "A simple global river bankfull width and depth database," Water Resour. Res. **49**, 7164–7168, https://doi.org/10.1002/wrcr.20440 (2013).
[44]T. M. Pavelsky, M. T. Durand, K. M. Andreadis, R. E. Beighley, R. C. Paiva, G. H. Allen, and Z. F. Miller, "Assessing the potential global extent of SWOT river discharge observations," J. Hydrol. **519**, 1516–1525 (2014).
[45]N. Catalán, R. Marcé, D. N. Kothawala, and L. J. Tranvik, "Organic carbon decomposition rates controlled by water retention time across inland waters," Nat. Geosci. **9**, 501–504 (2016).
[46]J. Bathurst, "Flow resistance through the channel network," Channel Network Hydrol. **19**, 69–98 (1993).
[47]L. C. Smith, B. L. Isacks, A. L. Bloom, and A. B. Murray, "Estimation of discharge from three braided rivers using synthetic aperture radar satellite imagery: Potential application to ungaged basins," Water Resour. Res. **32**, 2021–2034, https://doi.org/10.1029/96WR00752 (1996).
[48]D. M. Bjerklie, S. L. Dingman, C. J. Vorosmarty, C. H. Bolster, and R. G. Congalton, "Evaluating the potential for measuring river discharge from space," J. Hydrol. **278**, 17–38 (2003).
[49]L. C. Smith and T. M. Pavelsky, "Estimation of river discharge, propagation speed, and hydraulic geometry from space: Lena River, Siberia," Water Resour. Res. **44**, W03427, https://doi.org/10.1029/2007WR006133 (2008).
[50]R. P. M. Frasson, T. M. Pavelsky, M. A. Fonstad, M. T. Durand, G. H. Allen, G. Schumann, C. Lion, R. E. Beighley, and X. Yang, "Global relationships between river width, slope, catchment area, meander wavelength, sinuosity, and discharge," Geophys. Res. Lett. **46**, 3252–3262, https://doi.org/10.1029/2019GL082027 (2019).
[51]S. Cohen, A. J. Kettner, and J. P. Syvitski, "Global suspended sediment and water discharge dynamics between 1960 and 2010: Continental trends and intra-basin sensitivity," Global Planet. Change **115**, 44–58 (2014).
[52]J. D. Brown and G. B. Heuvelink, "Assessing uncertainty propagation through physically based models of soil water flow and solute transport," Encyclopedia Hydrol. Sci. (published online 2006).
[53]G. B. Heuvelink, *Error Propagation in Environmental Modelling with GIS* (CRC Press, 1998).
[54]R. F. Adler, G. Gu, M. Sapiano, J.-J. Wang, and G. J. Huffman, "Global precipitation: Means, variations and trends during the satellite era (1979–2014)," Surv. Geophys. **38**, 679–699 (2017).
[55]W. W. Immerzeel, L. P. Van Beek, and M. F. Bierkens, "Climate change will affect the Asian water towers," Science **328**, 1382–1385 (2010).
[56]E. Houghton, *Climate Change 1995: The Science of Climate Change: Contribution of Working Group I to the Second Assessment Report of the Intergovernmental Panel on Climate Change* (Cambridge University Press, 1996), Vol. 2.
[57]I. M. Held and B. J. Soden, "Robust responses of the hydrological cycle to global warming," J. Clim. **19**, 5686–5699 (2006).
[58]M. D. Dettinger and H. F. Diaz, "Global characteristics of stream flow seasonality and variability," J. Hydrometeorol. **1**, 289–310 (2000).
[59]C. Andermann, L. Longuevergne, S. Bonnet, A. Crave, P. Davy, and R. Gloaguen, "Impact of transient groundwater storage on the discharge of Himalayan rivers," Nat. Geosci. **5**, 127–132 (2012).
[60]C.-P. F. Hsu and J. M. Wallace, "The global distribution of the annual and semiannual cycles in precipitation," Mon. Weather Rev. **104**, 1093–1101, https://doi.org/10.1175/1520-0493(1976)104%3C1093:TGDOTA%3E2.0.CO;2 (1976).
[61]A. Behrangi, M. Christensen, M. Richardson, M. Lebsock, G. Stephens, G. J. Huffman, D. Bolvin, R. F. Adler, A. Gardner, B. Lambrigtsen *et al.*, "Status of high-latitude precipitation estimates from observations and reanalyses," J. Geophys. Res. **121**, 4468–4486, https://doi.org/10.1002/2015JD024546 (2016).
[62]B. Bookhagen and D. W. Burbank, "Toward a complete Himalayan hydrological budget: Spatiotemporal distribution of snowmelt and rainfall and their impact on river discharge," J. Geophys. Res. **115**, F03019, https://doi.org/10.1029/2009JF001426 (2010).
[63]M. Rajeevan, S. Gadgil, and J. Bhate, "Active and break spells of the Indian summer monsoon," J. Earth Syst. Sci. **119**, 229–247 (2010).
[64]K.-J. Ha, K.-Y. Heo, S.-S. Lee, K.-S. Yun, and J.-G. Jhun, "Variability in the East Asian monsoon: A review," Meteorol. Appl. **19**, 200–215 (2012).
[65]J. Zhou and K. Lau, "Does a monsoon climate exist over South America?," J. Clim. **11**, 1020–1040 (1998).
[66]J. Callow and G. Boggs, "Studying reach-scale spatial hydrology in ungauged catchments," J. Hydrol. **496**, 31–46 (2013).
[67]C. F. Byrne, G. B. Pasternack, H. Guillon, B. A. Lane, and S. Sandoval-Solis, "Reach-scale bankfull channel types can exist independently of catchment hydrology," Earth Surf. Processes Landforms **45**, 2179–2200 (2020).
[68]A. N. Strahler, "Quantitative analysis of watershed geomorphology," EOS, Trans. Am. Geophys. Union **38**, 913–920 (1957).
[69]A. Bejan, "The constructal law of organization in nature: Tree-shaped flows and body size," J. Exp. Biol. **208**, 1677–1686 (2005).
[70]A. Bejan and S. Lorente, "The constructal law of design and evolution in nature," Philos. Trans. R. Soc., B **365**, 1335–1347 (2010).
[71]A. Bejan and S. Lorente, "Constructal theory of generation of configuration in nature and engineering," J. Appl. Phys. **100**(5), 041301 (2006).
[72]D. Yamazaki, F. O'Loughlin, M. A. Trigg, Z. F. Miller, T. M. Pavelsky, and P. D. Bates, "Development of the global width database for large rivers," Water Resour. Res. **50**, 3467–3480, https://doi.org/10.1002/2013WR014664 (2014).
[73]F. Isikdogan, A. Bovik, and P. Passalacqua, "RivaMap: An automated river analysis and mapping engine," Remote Sens. Environ. **202**, 88–97 (2017).
[74]X. Yang, T. M. Pavelsky, G. H. Allen, and G. Donchyts, "RivWidthCloud: An automated Google Earth Engine algorithm for river width extraction from remotely sensed imagery," IEEE Geosci. Remote Sens. Lett. **17**, 217–221 (2019).
[75]K. Kirby, S. Ferguson, C. Rennie, I. Nistor, and J. Cousineau, "Assessments of available riverine hydrokinetic energy: A review," Can. J. Civil Eng. **49**, 839–854 (2021).
[76]IEC, "IEC TC 114: Marine energy—Wave, tidal and other water current converters," Tech. Report No. 62600-301 (International Electrotechnical Commission, 2018).
[77]J. Bomhof, "Estimating flow, hydraulic geometry, and hydrokinetic power at ungauged locations in Canada," Master's thesis (Université D'Ottawa/University of Ottawa, 2014).